

# TRANSLATIONAL ENERGY DISPOSAL AND MECHANISMS OF UNIMOLECULAR DISSOCIATIVE PHOTO-IONIZATION WITH He(I) AND Ne(I) RESONANCE LINES. A SURPRISAL ANALYSIS OF THE $\text{CH}_3\text{F} \rightarrow \text{CH}_3^+ + \text{F}$ PROCESS

J. MOMIGNY, R. LOCHT and G. CAPRACE

*Département de Chimie Générale et de Chimie Physique, Université de Liège, Institut de Chimie, Sart-Tilman par B-4000 Liège 1 (Belgium)*

## ABSTRACT

The He(I) and Ne(I) photo-ions translational energy spectra of  $\text{CH}_3^+$  from  $\text{CH}_3\text{F}$  were measured. At both wavelengths, the translational energy spectrum is made of two components. Their surprisal analysis shows two distinct behaviours: (i) the low energetic and narrow component exhibits a positive slope, whereas (ii) the high energetic and widely spread component is characterized by a negative slope. Furthermore, when the He(I) is used, the high translational energy distribution shows a multimodal surprisal. These observations as well as the origin of both distributions are discussed.

## INTRODUCTION

One of the main problems related to chemical dynamics is knowledge of the energy disposal between the products of a chemical reaction. In the unimolecular dissociation of molecular ions, two kinds of data are experimentally accessible: (i) the appearance energy and (ii) the translational energy distribution of the fragment ion produced in the process under investigation. Furthermore, the photo-electron-photo-ion coincidence technique (PIPECO), using rare gas resonance lines, allows a univocal assignment of the molecular ions' electronic states involved in the dissociation. It is also able, in some cases, to give important information about unimolecular decay kinetics of ions. For preset total excitation energies, the translational energy distribution of the fragment ions is derived from their time-of-flight (TOF) distributions. However, the analysis of the TOF distributions is usually based on a number of assumptions concerning the ion trajectories, the use of discrete and appropriately weighted translational energy values, the fit of the observed distribution by Maxwellian or exponential distribution functions.

The translational energy distributions reported in this paper have been determined by a retarding potential method, previously described [1] and used for the study of dissociative electro-ionization processes. The observed translational energy distribution has been compared to statistical distributions calculated by using the surprisal analysis reported by Levine and Bernstein [2]. As will be pointed out in this paper, the observation of bi- or multimodal surprisals, together with all the available experimental informations, will help to get a deeper view in the various mechanisms involved in the investigated dissociation process.

## EXPERIMENTAL

In the present fixed wavelength photo-ionization experiment, a newly built set-up is used and will be described elsewhere [3]. Briefly, the ions are produced by photo-ionization of molecules in the gas phase with vacuum UV light. The ionized species are extracted from the ionization region by a  $600 \text{ mV cm}^{-1}$  draw-out field. After leaving the ion source and before entering the quadrupole mass filter, the ions are energy-analyzed by means of a retarding lens, identical to that used in the electro-ionization experiment [1]. The retarding potential  $V_R$  is scanned by applying a voltage ramp to the retarding lens. The first derivative of the retarding potential curve is obtained numerically for energy intervals of typically 5 mV. However, the ion energy distributions, as presented in this work, are smoothed by taking the average value of the first derivative over an energy range of 50 mV.

The maximum of the  $\text{CH}_3\text{F}^+$  parent ions energy distribution is used as the zero energy calibration point for the ion translational energy scale.

## RESULTS

The total translational energy distributions  $P(E_T)$ , as observed with the Ne(I) and He(I) resonance lines,

were calculated from the observed  $\text{CH}_3^+$  ions energy distributions and are drawn in Figs. 1 and 2, respectively.

These distributions are compared to the a priori calculated statistical distributions  $P^0(E_T)$  evaluated by the method described in Appendix A of ref. 4 where the surprisal is defined by ref. 2 as

$$I(f_T) = -\ln \left[ \frac{P(E_T)}{P^0(E_T)} \right]$$

The a priori  $P^0(E_T)$  distribution is calculated in the Whitten-Rabinovitch approximation for the density of vibrational states of  $\text{CH}_3^+$ , using  $\nu_1(\text{I}) = 2400 \text{ cm}^{-1}$ ,  $\nu_2(\text{I}) = 1380 \text{ cm}^{-1}$ ,  $\nu_3(\text{II}) = 2560 \text{ cm}^{-1}$ , and  $\nu_4(\text{II}) = 1190 \text{ cm}^{-1}$ . These values are chosen by comparison with the wave numbers observed for the isoelectronic molecule  $\text{BH}_3$  [5]. For comparison, in  $\text{BH}_3$   $\nu_2 = (1560 + 50) \text{ cm}^{-1}$ , whereas in the  $\text{CH}_3^+$  ion  $\nu_2 = 1380 \text{ cm}^{-1}$ , as measured by He(I) photo-electron spectroscopy [6].

**Fig. 1.** Translational energy distribution of  $\text{CH}_3^+ + \text{F}$  from  $\text{CH}_3\text{F}$  induced by the Ne(I) resonance lines.

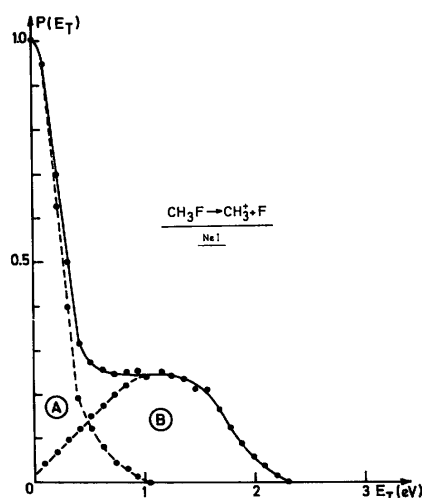
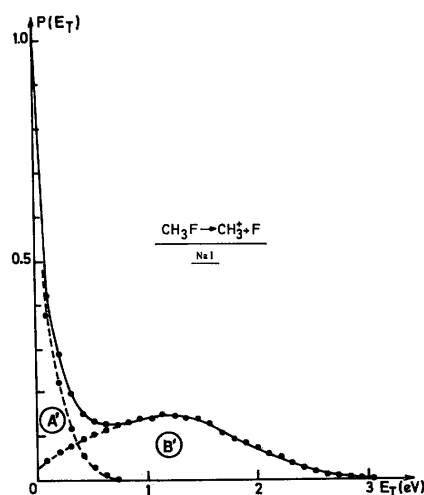


**Fig. 2.** Translational energy distribution of  $\text{CH}_3^+ + \text{F}$  from  $\text{CH}_3\text{F}$  induced by the He(I) resonance line.



The surprisal is expressed as a function of the reduced variable  $f_T = E_T/E$ , where  $E_T$  is the total translational energy and  $E$  is the maximum energy available for the considered process.  $I(f_T)$  is generally expressed by a straight line with a slope given by  $\lambda$ . In the present experiment,  $E$  is generally expressed by  $h\nu$ .

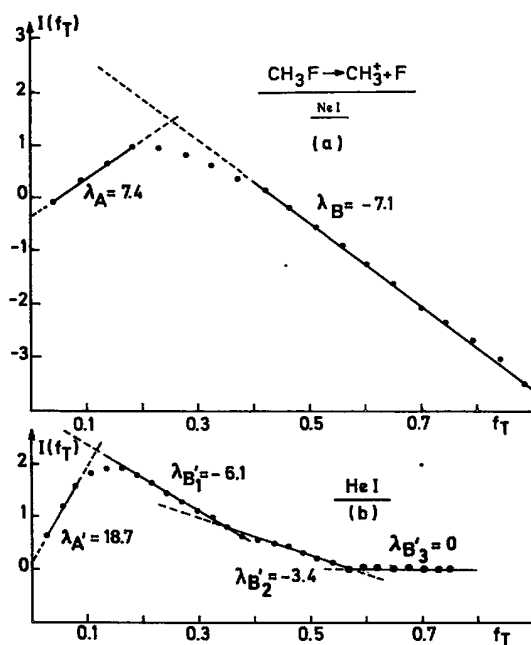
AE where  $h\nu$  is the ionizing photon energy and AE is the lowest thermodynamically calculated appearance energy for the dissociation process.

**TABLE 1.** Dissociation products of  $\text{CH}_3\text{F}^+$ , resulting electronic states and thermodynamic appearance energies used in this work

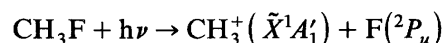
Dissociation products	Calculated A.E. (eV)	Resulting electronic states	
		$C_{3v}$	$C_s$
$\text{CH}_3^+(^1A_1) + \text{F}(^2P_u)$	14.58	$^2E, ^2A_1$	$^2A', ^2A'', ^2A'$
$\text{CH}_3(^2A''_2) + \text{F}^+(^3P_g)$	22.12	$^2E, ^4E, ^2A_2, ^4A_2$	
$\text{CH}_2\text{F}^+(^1A') + \text{H}(^2S_g)$	13.37		$^2A'$
$\text{CH}_2\text{F}^+(^3A'') + \text{H}(^2S_g)$	16.49 <sup>a</sup>		$^4A'', ^2A''$
$\text{CH}_2^+(^2A_1) + \text{HF}(^1\Sigma)$	14.10		$^2A'$
$\text{CH}_2(^3\Sigma_g^-) + \text{HF}^+(^2\Pi)$	20.20	$^2E, ^4E$	$^2A'', ^4A'', ^2A', ^4A'$

<sup>a</sup> The energy between  $\text{CH}_2\text{F}^+(^1A')$  and  $\text{CH}_2\text{F}^+(^3A'')$  is chosen as equal to that observed for the isoelectronic  $\text{H}_2\text{CO}$  molecule [10].

**Fig. 3.** Translational energy surprisal plots calculated for the whole  $\text{CH}_3^+$  ion energy distribution observed with (a) the Ne(I) resonance lines and (b) the He(I) resonance line.



However, in the He(I) photo-electron spectrum of  $\text{CH}_3\text{F}$  [7], the photon energy of  $h\nu = 21.22$  eV is strongly in excess with respect to the highest electronic state appearing in this energy range. Therefore, the  $h\nu$  value is chosen as given by the highest energy value of the last populated electronic state of  $\text{CH}_3\text{F}^+$ , i.e. 18.5 eV. On the other hand, when the Ne(I) radiation is used, the energy value  $h\nu$  is 16.85 eV. Referring to Table 1, the maximum available energy  $E$  for the process



is 3.92 and 2.27 eV for the He(I) and Ne(I) radiation, respectively.

The surprisal curves  $I(f_T)$  are given in Fig. 3. As was done for polymodal surprisals [8], the observed surprisal curves are interpreted by a series of linear portions.

The distributions  $A$  and  $A'$  in Figs. 1 and 2 are derived from the whole distribution by using the surprisal plot obtained for the distributions  $B$  and  $B'$  shown in Fig. 3(a) and (b).

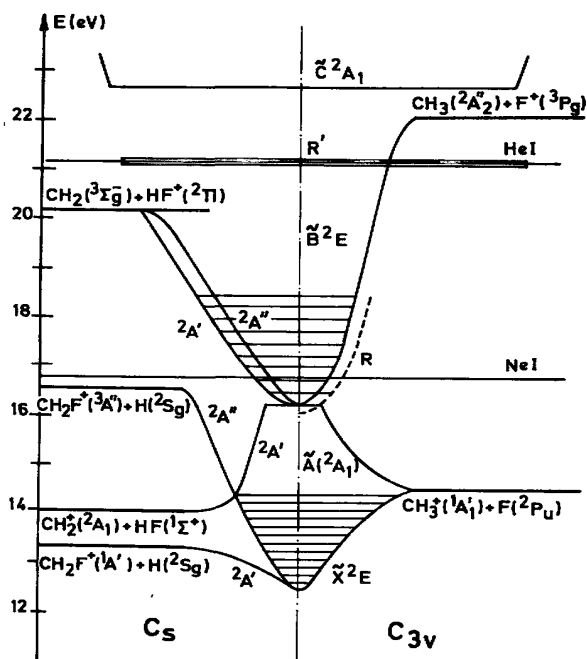
## DISCUSSION

The results will be discussed with the help of a tentative correlation diagram, shown in Fig. 4, based on the data collected in Table 1. The threshold energies given in this table have been calculated from the  $\Delta H_f^0$  value for each species as quoted in ref. 9.

*Mechanisms for the appearance of  $\text{CH}_3^+$ .* The horizontal lines in Fig. 4 shows the Franck-Condon population of the successive  $\text{CH}_3\text{F}^+$  electronic states, as excited by the He(I) resonance line. The PIPECO spectrum [11] shows that (a) the  $\text{CH}_3\text{F}^+$  ( $\tilde{X}^2E$ ) ground electronic state decays into  $\text{CH}_2\text{F}^+$  ions only, and (b) the  $\text{CH}_3\text{F}^+$  ( $\tilde{A}^2A_1 + \tilde{B}^2E$ ) excited electronic states, populated over the energy range of 16.25-18.5 eV, dissociate by  $\text{CH}_3^+$  ions production exclusively, with a rather wide translational energy distribution. Internal energy conversion from the  $\tilde{B}^2E$  state to the  $\tilde{A}^2A_1$  state is apparently total. Surprisingly, such internal energy conversion, giving rise to a large  $\text{CH}_3^+$  ion abundance, results in a very small  $\text{CH}_2^+$  ion intensity (below 0.5% of the total ionization).

The second parts  $B$  and  $B'$  of the translational energy distributions, observed in the present experiments either with the He(I) or the Ne(I) lines, agree rather well with the translational energy values observed with PIPECO spectroscopy [11] for excitation energies ranging from 16.25 eV up to 18.2 eV, i.e. close to the edge of the Franck-Condon region for the  $\text{CH}_3\text{F}^+$  ( $\tilde{B}^2E$ ) state population. Therefore, it will be considered that the distributions  $B$  and  $B'$  result from the direct population of the  $\text{CH}_3\text{F}^+$  ( $\tilde{A}^2A_1 + \tilde{B}^2E$ ) electronic states.

Fig. 4. Correlation diagram relative to the successive dissociation limits of  $\text{CH}_3\text{F}^+$ .



The lowest translational energy parts  $A$  and  $A'$  of the observed distributions are not observed in PIPECO experiments. For this reason, it is suggested that these are not produced by a direct dissociative ionization process giving rise to  $\text{CH}_3^+$  ions. The only alternative interpretation is the decay of  $\text{CH}_3\text{F}$  into  $\text{CH}_3^+ + \text{F}$  dissociation channel through the resonant excitation of suitable  $\text{CH}_3\text{F}$  neutral states.

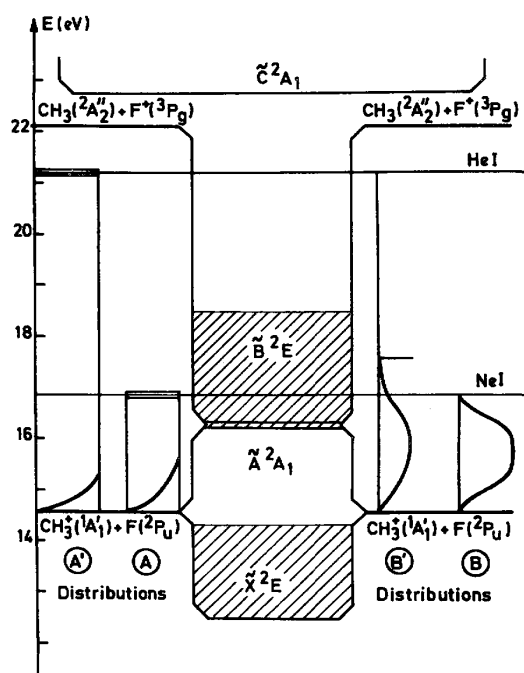
A good candidate for resonant excitation with the Ne(I) resonance Unes would be a Rydberg state  $R$ , member of a series converging to the  $\text{CH}_3\text{F}^+$  ( $\tilde{B}^2E$ ) state (see Fig. 4). With the He(I) resonance line, a Rydberg state  $R$  would be involved which would be a member of one of the series converging to the  $\text{CH}_3\text{F}^+$  ( $\tilde{C}^2A_1$ ) state

appearing at 22.5 eV [12]. These situations are represented in Fig. 5, together with the distributions *A*, *A'*, *B* and *B'*.

The autoionization process is most often associated with the appearance of zero or nearly zero translational energy electrons. If this is the case in the resonant population processes invoked for the *A* and *A'* distributions, the total excess energy is distributed between the translational energy of  $\text{CH}_3^+$  and F and the rovibrational energy of  $\text{CH}_3^+$ . It has to be pointed out that, if this interpretation does not imply any difficulty for the excitation with the Ne(I) lines, a problem arises when the resonant excitation through the He(I) line is involved. Indeed, the available total excess energy, in the latter condition, is  $21.22 - 14.58 = 6.64$  eV when  $E_T(\text{CH}_3^+ + \text{F}) = 0$  eV and about 5.9 eV when  $E_T(\text{CH}_3^+ + \text{F}) = 0.7$  eV, which is the maximum translational energy for the *A'* distribution. On the other hand, the maximum vibrational energy able to be stored in the  $\text{CH}_3^+$  ion up to the dissociation limit  $\text{CH}_3^+ \rightarrow \text{CH}_2^+ + \text{H}$  is 5.36 eV or  $\text{CH}_3^+ \rightarrow \text{CH}^+ + \text{H}_2$  is 5.42 eV. Consequently, with the He(I) line, the  $\text{CH}_3^+$  ions are thermodynamically allowed to decay at least to  $\text{CH}_2^+ + \text{H}$ . However, the  $\text{CH}_2^+$  ion abundance is very low in the He(I) mass spectrum (less than 0.5% of the total ionization).

Owing to the total absence of any detailed quantum mechanical description of the hypersurfaces of the  $\text{CH}_3\text{F}^+$  and the  $\text{CH}_3\text{F}^*$  systems, the explanation could only be conjectural. Either, for kinetic reasons, the dissociation of  $\text{CH}_3^+$  into smaller fragments is a rather uneasy process or, the electron emitted through autoionization has non-zero translational energy. Although no interpretation is put forward by the authors [7], an important and continuously distributed electron signal is detected in the range 18.5-21.2 eV in the He(I) photo-electron spectrum of  $\text{CH}_3\text{F}$ . Besides an instrumental artefact, autoionization could be the origin of these electrons.

**Fig. 5.** Schematic correlation diagram showing the probable origin of the *A*, *A'*, *B* and *B'* translational energy distributions. The *A* distributions are due to the decay of resonantly excited neutral states of  $\text{CH}_3\text{F}$  either by Ne(I) (*A* distribution) or by He(I) (*A'* distribution). Therefore, they are not detected by PIPECO experiments. The *B* distributions are produced by the direct excitation of the  $\text{CH}_3\text{F}^+$  ( $\tilde{A} + \tilde{B}$ ) states and are similar to those observed in PIPECO experiments [11].



*Discussion of the surprisal plots.* Figure 3(a) and (b) clearly show that the translational energy surprisal for the distributions *A* and *A'* plotted vs. the reduced energy  $f_T$  has a positive slope. The result displayed in Fig. 3(b), calculated for a maximum available energy  $E = 3.92$  eV, does not differ appreciably for  $E = 6.64$  eV; the slope remains positive.

Both distributions are interpreted as being due to the indirect population of the dissociation limit through the resonant excitation of high-Rydberg states.

If the rotational energy distribution is not too surprising, the positive slope found for the production of low energy  $\text{CH}_3^+$  ions with either the He(I) or Ne(I) Unes, implies that a *population inversion of the simultaneously produced vibrational levels of  $\text{CH}_3^+$*  is expected.

The surprisal plot for the  $B$  and the  $B'$  distributions mainly shows a negative slope. These distributions are ascribed to the  $\text{CH}_3^+$  ions production through the direct population and dissociation of the  $\text{CH}_3\text{F}^+(\tilde{A}^2A_1 + \tilde{B}^2E)$  states.

When the Ne(I) lines are used, the measured translational energy has a maximum width corresponding to the excess energy involved in the process. Only 20% of the Franck-Condon allowed population of the  $\text{CH}_3\text{F}^+(\tilde{A}^2A_1 + \tilde{B}^2E)$  states are involved. The surprisal plot shows only one negative slope of  $\lambda_B = -7.1$  [see Fig. 3(a)].

However, when the He(I) resonance line is used, 100% of the Franck-Condon allowed population of these states is involved. The energy increase of 1.65 eV, between the maximum energy of the Ne(I) resonance lines (16.85 eV) and the upper edge of the  $\text{CH}_3\text{F}^+(\tilde{A} + \tilde{B})$  band (18.5 eV), corresponds to a translational energy increase of only 0.7 eV. Furthermore, this energy increment contributes to only a small part of the  $\text{CH}_3^+$  ion intensity, whereas the  $\text{CH}_3\text{F}^+(\tilde{A}^2A_1 + \tilde{B}^2E)$  ionization cross-section is five times larger than with the Ne(I) lines.

This additional part of the  $\text{CH}_3^+$  ions translational energy distribution corresponds to a zero slope ( $\lambda_{B3} = 0$ ) in the surprisal plot. This would mean that when the whole  $\text{CH}_3\text{F}^+(\tilde{A}^2A_1 + \tilde{B}^2E)$  state is populated in the Franck-Condon region, the time needed for the redistribution of the available total electronic energy is such that at least a fraction of the process leads to a statistical redistribution of the excess energy.

Furthermore, this situation is also reflected in the remaining part of the translation energy distribution, coinciding with that observed with the Ne(I) lines. Though being negative, the slope of the surprisal plot is bimodal and less negative ( $\lambda_{B1} = -6.1$  and  $\lambda_{B2} = -3.4$ ) than the monomodal surprisal observed with Ne(I) ( $\lambda_B = -7.1$ ).

In a previous electro-ionization work on the dissociative ionization of  $\text{CH}_3\text{F}$  [13], the onset energy of  $\text{CH}_3^+$  as a function of its kinetic energy has been examined. This study unambiguously showed a jump from 16.5 eV to 17.1 eV for the appearance energy of  $\text{CH}_3^+$  for a translational energy of 1.4-1.5 eV. This latter energy corresponds to about  $f_T = 0.63$  and was ascribed to the contribution of the  $\text{CH}_3\text{F}^+(\tilde{B}^2E)$  state.

The present surprisal analysis at least shows that the  $\text{CH}_3^+$  ions at the end of the translational energy distribution observed with He(I) behave distinctly from those  $\text{CH}_3^+$  ions of lower energy and from those observed with the Ne(I) resonance lines.

These differences evidence a change in the dissociation dynamics when the translational energy distribution results from the entire Franck-Condon population of the  $\text{CH}_3\text{F}^+(\tilde{A}^2A_1 + \tilde{B}^2E)$  band. The negative slopes in the surprisal plot will further evidence that *the vibrational distribution of  $\text{CH}_3^+$  will not be statistical and also not inverted.*

## CONCLUSIONS

The translational energy distributions of  $\text{CH}_3^+$  ions, induced in  $\text{CH}_3\text{F}$  by either Ne(I) or He(I) resonance lines, show two components.

The first distribution, not observed by PIPECO, peaks at zero translational energy and extends up to 1 eV with Ne(I) or 0.7 eV with He(I). The corresponding  $\text{CH}_3^+$  ions are produced by the indirect population of the dissociation limit  $\text{CH}_3^+(\tilde{X}^1A_1) + \text{F}(^2P_u)$  through the decay of Rydberg states excited by both the He(I) and Ne(I) resonance lines. Furthermore, to these distributions corresponds a positive slope of the translational energy surprisal which correlates with a population inversion in the vibrational energy distribution of the  $\text{CH}_3^+$  ions.

The second distribution, identical to that observed by PIPECO, results from the direct population and decay of the  $\text{CH}_3\text{F}^+(\tilde{A}^2A_1 + \tilde{B}^2E)$  states. The negative slope of the translational energy surprisal evidences a non-statistical and non-inverted vibrational energy distribution of the  $\text{CH}_3^+$  ions. This slope is monomodal in the

Ne(I) ion energy spectrum and multimodal in the He(I) spectrum. Although the exploration of a larger part of the phase space does not appreciably modify the distribution when the He(I) line is used, the multimodal behaviour has to be related to the more complex dynamics of the dissociation process.

## **ACKNOWLEDGEMENTS**

The financial support of the Université de Liège, the Fonds de la Recherche Fondamentale Collective and the Belgian Government through the Action de Recherche Concertée allowed these experiments to be carried out. We wish to thank these foundations for their support.

## **REFERENCES**

- 1 R. Locht and J. Schopman, *Int. J. Mass Spectrom. Ion Phys.*, 15 (1974) 361.
- 2 R.D. Levine and R.B. Bernstein, *Ace. Chem. Res.*, 7 (1974) 393.
- 3 R. Locht and J. Momigny, to be published.
- 4 J. Momigny, R. Locht and G. Caprace, *Chem. Phys.*, 102 (1986) 275.
- 5 J.R. Morray, A.B. Johnson, Y.C. Fu and G.R. Hull, in R.G. Gould (Ed.), *Chem. Ser.* 32 (1961) 157.
- 6 J. Dyke, N. Jonathan, E. Lee and A. Morris, *J. Chem. Soc. Faraday Trans. 2*, 72 (1976) 1385.
- 7 L. Karlsson, R. Jadrny, L. Mattsson, F.T. Chau and K. Siegbahn, *Phys. Scr.*, 16 (1977) 225.
- 8 A. Ben Shaul, R.D. Levine and R.B. Berstein, *J. Chem. Phys.*, 57 (1972) 5440.
- 9 H.M. Rosenstock, K. Draxl, B.W. Steiner and J.T. Herron, *J. Phys. Chem. Ref. Data Suppl.* 1, 6 (1977).
- 10 G.W. Robinson and V.E. Giorgio, *Can. J. Chem.*, 36 (1958) 31.
- 11 J.H.D. Eland, R. Frey, A. Kuestler, H. Schulte and B. Brehm, *Int. J. Mass Spectrom. Ion Phys.*, 22 (1976) 155.
- 12 G. Bieri, L. Åsbrink and W. Von Niessen, *J. Electron Spectrosc. Relat. Phenom.*, 23 (1981) 281.
- 13 R. Locht and J. Momigny, *Int. J. Mass Spectrom. Ion Processes*, 71 (1986) 141.